Artificial Life and Robotics (2024) 29:55–61
https://doi.org/10.1007/s10015-023-00935-2

ORIGINAL ARTICLE

Design of effective suction force sensible vacuum gripper by a 6-axis force sensor

Sou Izumi[1] · Shuhei Ikemoto[1]

Received: 31 August 2023 / Accepted: 15 December 2023 / Published online: 19 January 2024

Abstract

This study proposes a vacuum gripper that can measure the effective suction force applied to an object using a 6-axis force sensor. The object falling in a vacuum gripper occurs when a gap between the object and the pad no longer allows the negative pressure in the chamber. This is rephrased as the absence of a compression force between the object and the pad. Therefore, the force distribution that the attached object pushes the pad during suction reflects the external force, i.e. the effective suction force, required to remove the object. To confirm the validity of the developed vacuum gripper, we conducted an experiment where the developed vacuum gripper sucks a flat plate. As a result, we confirmed that the 6-axis force sensor's signals mean the effective suction force by applying an external force to remove the place.

Keywords Vacuum gripper · Force sensor · Effective suction force

1 Introduction

Dexterous grasping and manipulation is one of the most traditional and challenging problems in robotics. The development of tactile sensors and their integration into end-effectors has been the key to solving this problem. For example, a wide variety of tactile sensors have been proposed [1], including those that use the piezoelectric effect [2], piezoresistive effect [3], contact resistance [4], changes in magnetic flux density [5], and observation of changes in light intensity and wavelength [6–10]. In other words, tactile sensors do not have a unified and standardized physical quantity to be measured, such as 6-axis force sensors. This diversity of tactile sensors makes it difficult to clarify and standardize applying tactile information to end-effectors. Therefore, for constructing a methodology to utilize tactile information, it is helpful to use standardized sensors and integrate them into an end-effector that exploits simple mechanics between the grasped object and the end-effector.

The vacuum gripper is one of the most practical end-effectors for wide variety of application [11, 12]. The mechanics between the gripper and the end-effector is simple because the negative pressure produces a normal force on the attached object's surface [13]. Specifically, the falling of an attached object in a vacuum gripper occurs when the gap between the object and the periphery of the pad becomes sufficiently large that the incoming air cannot maintain the negative pressure. In other words, the force distribution of the attached object pushing against the pad periphery during suction directly expresses the external force required to drop the object. However, most studies on vacuum suction have focused on how well the object conforms to non-flat surfaces, and there have been few attempts to incorporate tactile sensors to measure the distribution of pushing force on the periphery of the pad [14, 15]. If we can incorporate a tactile sensor into vacuum suction and measure the effective suction force acting on the object to hold it, the quality of the suction may be evaluated independent of the type of object due to its simple mechanics.

In this study, we focus on a 6-axis force sensor as a well-standardized sensor and a vacuum gripper as an end-effector based on simple mechanics and develop a vacuum gripper that

This work was submitted and accepted for the Journal Track of the joint symposium of the 29th International Symposium on Artificial Life and Robotics, the 9th International Symposium on BioComplexity, and the 7th International Symposium on Swarm Behavior and Bio-Inspired Robotics (Beppu, Oita and Online, January 24–26, 2024).

✉ Shuhei Ikemoto
ikemoto@brain.kyutech.ac.jp

[1] Kyushu Institute of Technology, Graduate School of Life Science and Systems Engineering, 2-4 Hibikino, Wakamatsu, Kitakyushu, Fukuoka 808-0196, Japan

can measure the effective suction force. In the next section, we first describe the design and implementation of the developed vacuum suction pad. In the third section, the experiments conducted to evaluate the vacuum gripper are described, and the usefulness of the developed vacuum gripper is demonstrated based on the results obtained. Finally, the possibility of new motion planning and control using the developed vacuum gripper will be discussed, and future works will be described.

2 Proposed vacuum gripper

2.1 Principle and design

We define the effective suction force as the minimum external force required to break the suction as the object moves perpendicular to the suction surface. In particular, note the following characteristics:

1. The effective suction force equals the force/torque the attached object pushes against the vacuum gripper's surface. It reflects the influence of both external forces applied to the attached object and changes in the negative pressure.
2. The total suction force as the product of the pressure difference and the pressure-receiving area does not reflect the presence or absence of an external force applied to the attached object and thus differs from the effective suction force.
3. The mass of the attached object does not reflect changes in the negative pressure and thus is different from the effective suction force.

Referring to these features and specifications, the vacuum gripper developed in this research uses a 6-axis force sensor to measure the effective suction force.

Figure 1 shows a schematic of the mechanical equilibrium during object suction. Defining the local z-axis to express the suction force direction. Considering a plane parallel to the z-axis, namely the suction force direction, passing through the center of negative pressure and the object's center of gravity, All representative forces relating to suction are aligned on the xi-axis orthogonal to the z-axis. The F_s and F_e represent the total suction force and the external force. The reaction forces F_{r1} and F_{r2} act to stabilize the object under the influence of F_s and F_e as follows:

$$F_{r1} = -\frac{F_s}{2} + \frac{l-r}{2r}F_e \tag{1}$$

$$F_{r2} = -\frac{F_s}{2} - \frac{l_r}{2r}F_e \tag{2}$$

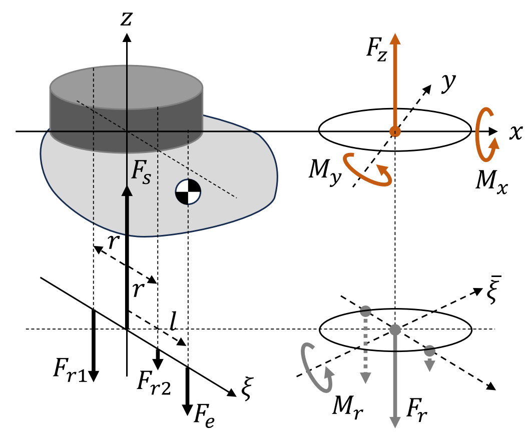

Fig. 1 Schematic of the mechanical equilibrium during object suction. Left: The mechanical equilibrium in a plane parallel to the z-axis passing through the center of negative pressure and the object's center of gravity. Bottom right: The reaction force at the negative pressure center and the reaction moment around the axis perpendicular to the plane. Top right: The force/torque measured from the vacuum gripper's reference frame (top right)

where $F_s > 0$, $F_{r1} < 0$, and $F_{r2} < 0$ hold while the suction is maintained. Therefore, while the suction is maintained in this simple model, the effective suction force $\hat{F}$ is defined as follows:

$$\hat{F} = \max(|F_{r1}|, |F_{r2}|). \tag{3}$$

In addition, the F_{r1} and F_{r2} can be written by the reaction force at the negative pressure center F_r and the reaction moment M_r around the axis orthogonal to the ξ–z plane:

$$F_r = F_{r1} + F_{r2} \tag{4}$$

$$M_r = (F_{r1} - F_{r2})r. \tag{5}$$

The force/torque sensor measures F_r and M_r from the vacuum gripper's reference frame. In this simple model, the F_z, M_x, and M_y have following relationships with F_r and F_r.

$$F_r = -F_z \tag{6}$$

$$M_r = \sqrt{{M_x}^2 + {M_y}^2}. \tag{7}$$

Figure 2 shows a schematic of the developed vacuum gripper's design. The Conventional Vacuum Gripper in Fig. 1 depicts the vacuum gripper's structure widely used today. The working principle is extremely simple. By depressurizing the chamber formed by the attached object and the vacuum gripper, a force equivalent to the product of the pressure difference and the pressure-receiving area, namely the total suction force, is generated, and suction is

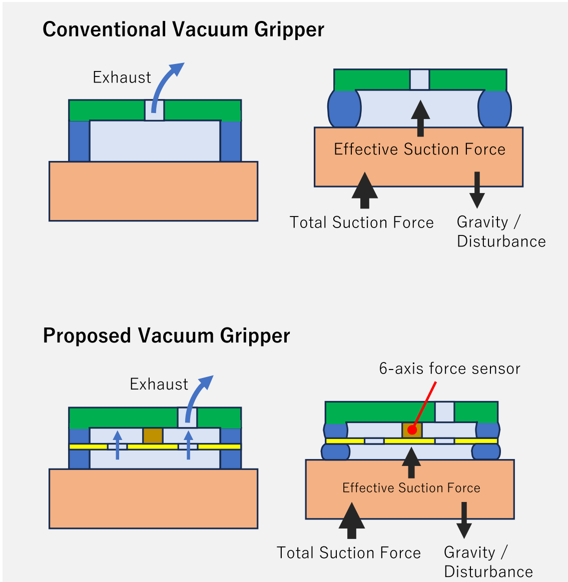

Fig. 2 Schematic of the proposed vacuum gripper's working principle. The upper row shows the conventional vacuum gripper, and the lower row shows the proposed one. The vacuum gripper generates a suction force on the attached object in the direction of the rigid plate (yellow) by depressurizing the chamber (light blue) formed by the rigid plate, the periphery (blue), and the object (orange). A 6-axis force sensor is installed between the rigid plate and the base frame (green) (color figure online)

performed. The periphery of the vacuum gripper deforms to maintain the chamber airtight and supports the attached object. To hold the attached object firmly, the total suction force has to be effectively larger than gravity and disturbance applied on the attached object. The effective suction force means this difference, the minimum external force required to break the suction as the object moves perpendicular to the suction surface. The effective suction force has not been measured or estimated to our best knowledge.

The Proposed Vacuum Gripper in Fig. 1 aims to measure the effective suction force by a 6-axis force sensor. A rigid plate is added to divide the deforming periphery, and a 6-axis force sensor is mounted between the plate and the base frame of the vacuum gripper. The rigid plate has holes that allow air to pass through. To let the force sensor primarily support the force applied between these two rigid bodies, the periphery surrounding the force sensor is designed to be flexible but airtight. On the other hand, the role of the periphery that touches the attached object is the same as that of the conventional vacuum gripper. The position of this force sensor is intended to measure the force of the attached object pushing the base frame through the periphery. Therefore, the proposed vacuum gripper measures the effective suction force directly.

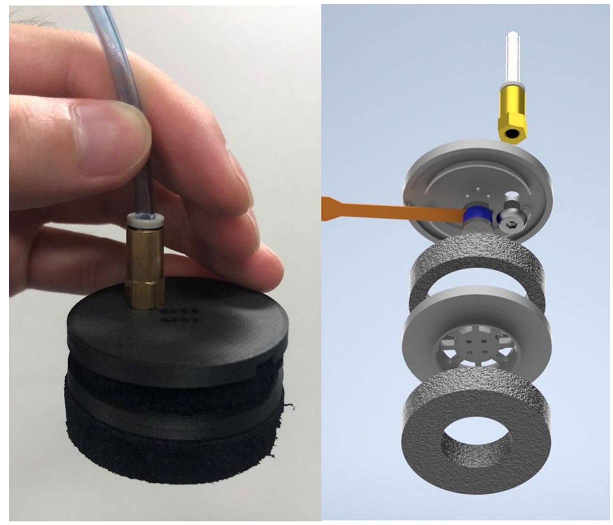

Fig. 3 Developed vacuum gripper. Left: The overview of the developed vacuum gripper. The base frame and the rigid plate are fabricated using a 3D printer with a carbon fiber-reinforced material filament. For the soft periphery, a sponge is used. Right: The design of the developed vacuum gripper. A miniature 6-axis force sensor (MMS101, MinebeaMitsumi, Inc.) is installed between the base frame and the rigid plate

2.2 Developed vacuum gripper

Based on the working principle explained in Fig. 2, we developed a vacuum gripper equipped with a small 6-axis force sensor. Figure 3 shows the developed vacuum gripper's overview and design. The developed vacuum gripper has an outer diameter of 46 mm, a height of 24 mm, and a mass of 25 g. The diameter of the circular pressure-receiving area where the negative pressure acts is approx. 20 mm. It is not closed-cell foam, and the airtightness is not assured but practically usable as the periphery. A miniature 6-axis force sensor (MMS101, MinebeaMitsumi, Inc) is installed between the base frame and the rigid plate. Its outer diameter, height, and mass are 9.6 mm, 9.0 mm, and 3 g, respectively. Despite its extremely small size, the rated load, the rated torque, the load capacity, and the torque capacity are 40 N, 0.4 N m, 200 N, and 1.8 N m, respectively. Both end faces of the 6-axis force sensor are screwed to the base frame and the rigid plate. A conventional conductive polyethylene sponge is sandwiched between the base frame and the rigid plate to maintain the airtightness inside the vacuum gripper. This sponge is as soft as the sponge utilized at the periphery of commercially available vacuum grippers and is not strictly airtight. All other parts are assembled by simply fitting them together because suction force will be applied to tighten them.

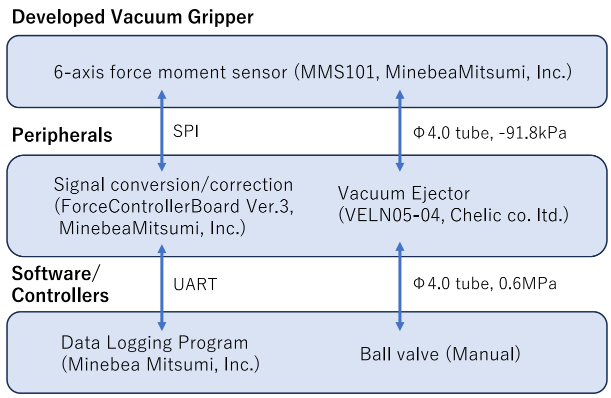

Fig. 4 System architecture of the developed vacuum gripper. The developed vacuum gripper has a miniature 6-axis force sensor (MMS101, MinebeaMitsumi, Inc). The negative pressure for vacuum suction is generated by a vacuum ejector (VELN05-04, Chelic Co. Ltd.)

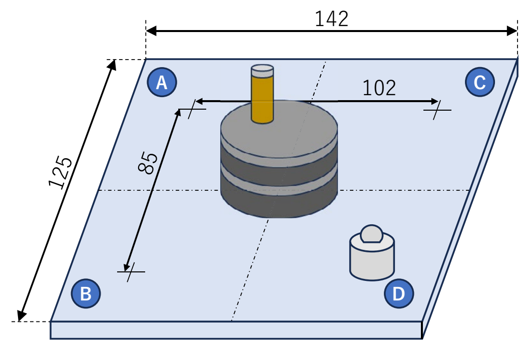

Fig. 5 Experimental setup. After the plate is sucked and lifted, a weight with a mass of 10 g and 20 g is placed at the four corners of the plate, indicated by A to D, sequentially and alternately

2.3 System architecture

Figure 4 shows the system architecture of the developed vacuum gripper. The system is simple since this study aims to validate the developed vacuum gripper. The 6-axis force sensor provides information via SPI, and a peripheral board receives signals and converts them into 6-axis force and torque. The measured force/torque is sent to a host computer via UART and stored in CSV format. The negative pressure for vacuum suction is generated by a vacuum ejector (VELN05-04, Chelic Co. Ltd.). Vacuum suction is performed manually using a ball valve.

3 Experiment

To validate the developed vacuum gripper, we conducted an experiment to confirm the following features:

1. Whether or not force/torque changes can be measured when the vacuum gripper sucks an attached object.
2. Whether or not the weight of the attached object is reflected in the force/torque when it is lifted.
3. Whether or not it is possible to identify where and how much disturbance has occurred.

By definition of the effective suction force stated in Sect. 2.1, confirming all features indicates that the developed vacuum gripper can successfully measure the effective suction force.

3.1 Experimental setup

Figure 5 shows the experimental setup for confirming three aforementioned features in the developed vacuum gripper. In the experiment, the center of a plate 142 mm long, 125 mm wide, and 50 g in mass is suctioned by the developed vacuum gripper. First, the plate pushes against the periphery of the vacuum gripper due to suction. If the 6-axis force sensor can observe this effect, the feature described in 1 above can be confirmed. Next, when the suctioned plate is lifted, a force equivalent to the weight of the plate pulls the periphery. If this effect can be observed, we can confirm that the developed vacuum gripper has the feature described in 2 above. Finally, by placing weights of different masses at different locations on the plate in sequence, if the feature described in 3 above exists, the measured force/torque will reflect information on where and how much force is applied.

3.2 Results

The graph in Fig. 6 shows the change in the force in the direction that the object pushes the vacuum gripper, as measured by the 6-axis force sensor, from before the suction to after sucking the object. As shown in the pictures in the upper row of Fig. 6, the deformation of the developed vacuum gripper before and after the suction cannot be visually confirmed. On the other hand, the suction effect can be observed in the graph. This supports that the developed vacuum gripper holds feature 1 explained in Sect. 3.1.

The suction force can be estimated by $\pi d^2 P/4$. From the design of the developed vacuum gripper, the theoretical suction force is calculated as approx. 30 N. However, the actual suction force measured in this result is approx. 3 N. As explained in Sect. 2.2, the developed vacuum gripper is assembled by snapping on all parts without gluing. Therefore, this decrease in the suction force can be attributed to air leakage, mainly between rigid parts and the sponge surrounding the force sensor.

The graph in Fig. 7 shows the change in the force in the direction that the object pushes the vacuum gripper, as measured by the 6-axis force sensor, from just after

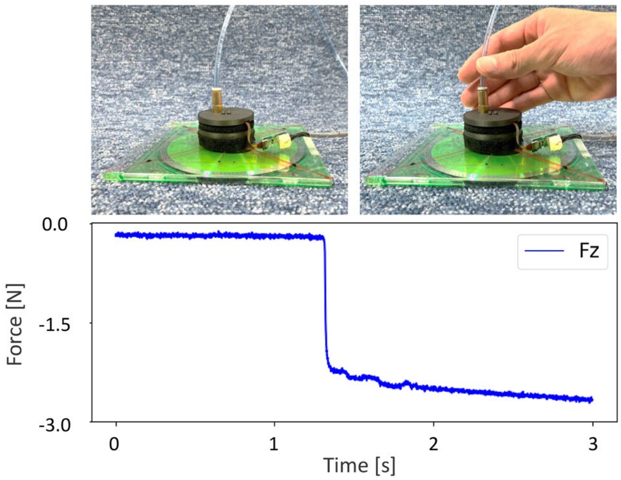

Fig. 6 Changes in the force exerted in the direction that the object pushes the vacuum gripper when the suction starts. The 6-axis force sensor on the developed suction gripper measured the force. A suction force of approximately 3 N, which is about 10% of the theoretical suction force, was measured

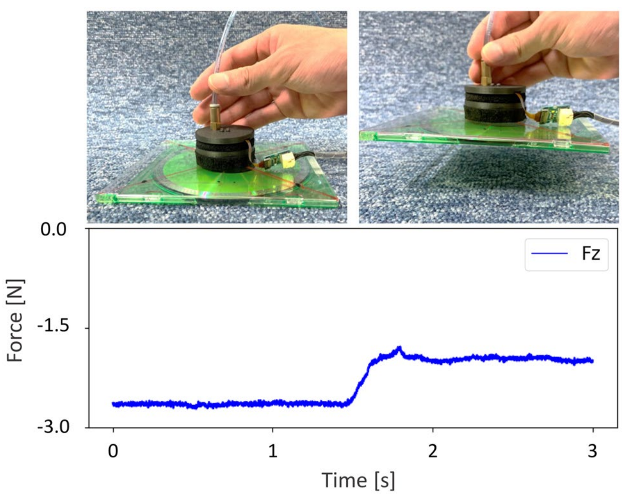

Fig. 7 Changes in the force exerted in the direction that the object pushes the vacuum gripper when the attached object is lifted. Lifting the object reduced the suction force by about 0.5 N. Because the object's mass is 50 g, this can be interpreted as a reduction in effective suction force by the object's weight

sucking the object to after lifting the object. This operation is thought to reduce the effective suction force by the weight of the attached object. As explained in Fig. 5, the mass of the rigid plate attached to the developed vacuum gripper is 50 g. Therefore, the expected reduction of the effective suction force is estimated as approx. 0.5 N. As indicated by this estimate, the suction force in the bottom row of the graph in Fig. 7 was reduced by approx. 0.5 N. This supports that the developed vacuum gripper holds the feature 2 explained in Sect. 3.1.

Figures 8, 9 and 10 show the changes in torque when weights of 5 g, 10 g, and 20 g are placed at positions A to D shown in Fig. 4, respectively. In each figure, the positive and negative torques around the orthogonal *x*- and *y*-axes identify where the weight is placed in each of the four positions. The composite moments calculated by Eq. 7 were approximately 0.0014, 0.0022, and 0.0055 N m in Figs. 8, 9 and 10, respectively. Their theoretical values are 0.0033, 0.0065, and 0.013 N m (the moment arm is about 66.4 mm), indicating that the heavier the weight, the larger the error. While the deformation of the sponge due to the weight is not taken into account in the simple theoretical model, in the experiment, the deformation of the sponge causes the gripping object to tilt. Therefore, the heavier the weight, the larger the deformation, and the larger the difference between the theoretical and measured values. On the other hand, a comparison of these figures shows that the mass of the placed weight can be clearly identified from the magnitude of the torque. This supports that the developed vacuum gripper holds feature 3 explained in Sect. 3.1, and it is confirmed that the developed vacuum gripper has all three features.

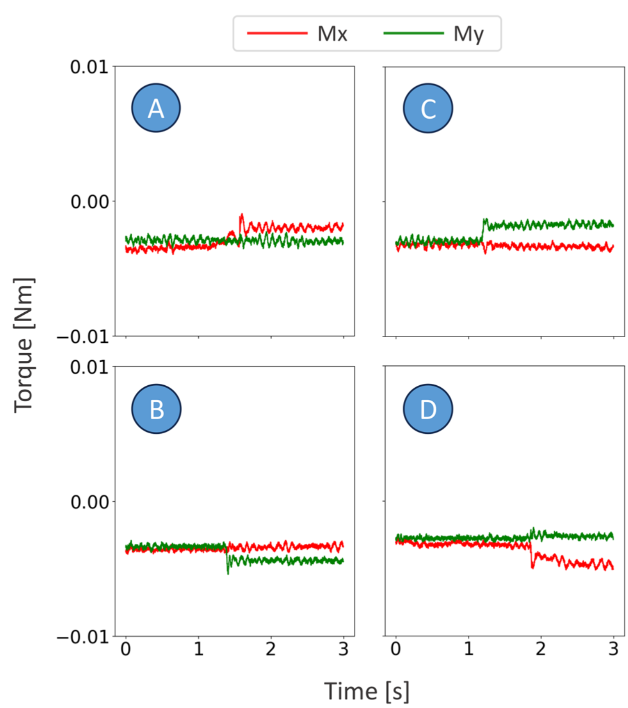

Fig. 8 Changes in the torque around the *x*-axis and *y*-axis when a 5 g weight is placed in the four positions in sequence. The positive and negative changes in the torque around the *x*-axis and *y*-axis can identify where the weight is placed in each of the four positions

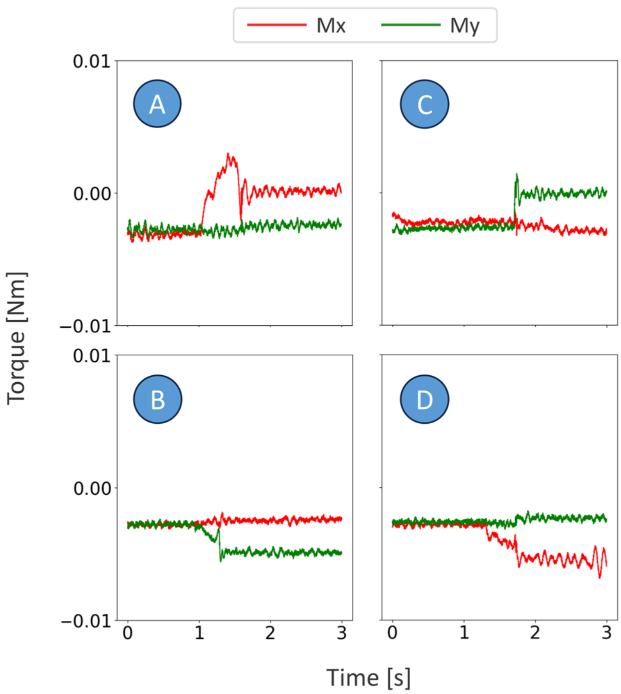

Fig. 9 Changes in the torque around the *x*-axis and *y*-axis when a 10 g weight is placed in the four positions in sequence. The positive and negative changes in the torque around the *x*-axis and *y*-axis can identify where the weight is placed in each of the four positions

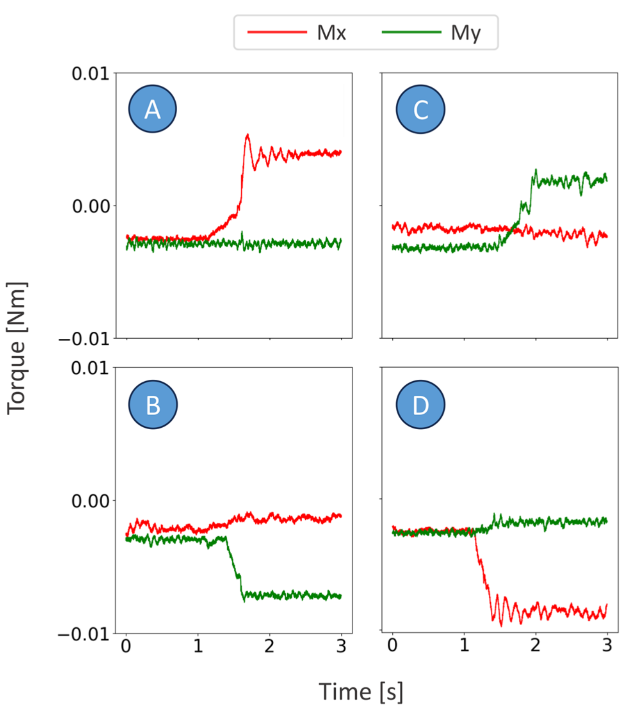

Fig. 10 Changes in the torque around the *x*-axis and *y*-axis when a 20 g weight is placed in the four positions in the sequence. The positive and negative changes in the torque around the *x*-axis and *y*-axis can identify where the weight is placed in each of the four positions

4 Conclusion and future work

In this study, we proposed a vacuum gripper that can measure an effective suction force by a 6-axis force sensor. The effective suction force was defined as the minimum external force required to break the suction as the object moves perpendicular to the suction surface. After explaining the specific implementation of the developed suction gripper, the design of experiments for confirming that it can measure the effective suction force was explained. The experiments validated that the developed vacuum gripper can measure the effective suction force by the mounted 6-axis force sensor.

For future prospects, we will discuss improvements to the device and possibilities for motion planning. In this experiment, the effective suction force was smaller than their theoretical values, which can be caused by the lack of air-tightness in the vacuum gripper. In particular, we believe that the cause is air leakage from the sponge between the object and the rigid plate, as well as between the rigid plate and the base frame. In the design we developed, the conductive sponge is not adhered to either the rigid plate or the base frame. Additionally, the mechanical properties of this sponge are not fully public and there is no mention about its airtightness. Therefore, we plan to investigate the aforementioned contact surfaces where air leakage may occur and update the design and the implementation to improve their airtightness. Due to this change, we expect the measured values to come closer to the theoretical values.

Furthermore, using the torque and force information from the 6-axis force sensor makes it possible to estimate the distribution of forces pushing against the periphery of the pad, allowing for a more appropriate assessment of the effective suction force. Based on this quantitative information regarding the risk of falling, we are considering planning the optimal trajectory for the robotic arm, tailored to the suction conditions of the object being vacuumed. In this challenge, D'Alembert's principle allows the ideas in this paper to be extended to dynamic problems in which objects are subject to inertial forces. Extension to dynamic problems is an important future work for this research.

Acknowledgements This work was supported by JSPS KAKENHI Grant Numbers 19K0285, 19H01122, and 21H03524.

Data availability The datasets generated and/or analyzed during the current study are available in the GitHub repository: [https://github.com/BSL-Kyutech/izumi2024design.git].

References

1. Pyo S, Lee J, Bae K, Sim S, Kim J (2021) Recent progress in flexible tactile sensors for human-interactive systems: from sensors to advanced applications. Adv Mater 33(47):2005902
2. Lin W, Wang B, Peng G, Shan Y, Hong H, Yang Z (2021) Skin-inspired piezoelectric tactile sensor array with crosstalk-free row+column electrodes for spatiotemporally distinguishing diverse stimuli. Adv Sci 8(3):2002817
3. Wisitsoraat A, Patthanasetakul V, Lomas T, Tuantranont A (2007) Low cost thin film based piezoresistive mems tactile sensor. Sens Actuators A: Phys 139(1):17–22
4. Zhang J, Zhou LJ, Zhang HM, Zhao ZX, Dong SL, Wei S, Zhao J, Wang ZL, Guo B, Hu PA (2018) Highly sensitive flexible three-axis tactile sensors based on the interface contact resistance of microstructured graphene. Nanoscale 10(16):7387–7395
5. Kawasetsu T, Horii T, Ishihara H, Asada M (2018) Flexible tri-axis tactile sensor using spiral inductor and magnetorheological elastomer. IEEE Sens J 18(14):5834–5841
6. Yamaguchi A, Atkeson CG (2016) Combining finger vision and optical tactile sensing: reducing and handling errors while cutting vegetables. In: 2016 IEEE-RAS 16th international conference on humanoid robots (Humanoids). IEEE, Mexico, pp 1045–1051
7. Yuan W, Dong S, Adelson EH (2017) Gelsight: high-resolution robot tactile sensors for estimating geometry and force. Sensors 17(12):2762
8. Donlon E, Dong S, Liu M, Li J, Adelson E, Rodriguez A (2018) Gelslim: a high-resolution, compact, robust, and calibrated tactile-sensing finger. In: 2018 IEEE/RSJ international conference on intelligent robots and systems (IROS). IEEE, Spain, pp 1927–1934
9. Hughes D, Lammie J, Correll N (2018) A robotic skin for collision avoidance and affective touch recognition. IEEE Robot Autom Lett 3(3):1386–1393
10. Koyama K, Shimojo M, Senoo T, Ishikawa M (2018) High-speed high-precision proximity sensor for detection of tilt, distance, and contact. IEEE Robot Autom Lett 3(4):3224–3231
11. Fujita M, Ikeda S, Fujimoto T, Shimizu T, Ikemoto S, Miyamoto T (2018) Development of universal vacuum gripper for wall-climbing robot. Adv Robot 32(6):283–296
12. Matsuo I, Shimizu T, Nakai Y, Kakimoto M, Sawasaki Y, Mori Y, Sugano T, Ikemoto S, Miyamoto T (2020) Q-bot: heavy object carriage robot for in-house logistics based on universal vacuum gripper. Adv Robot 34(3–4):173–188
13. Mantriota G (2007) Theoretical model of the grasp with vacuum gripper. Mech Mach Theory 42(1):2–17
14. Aoyagi S, Suzuki M, Morita T, Takahashi T, Takise H (2020) Bellows suction cup equipped with force sensing ability by direct coating thin-film resistor for vacuum type robotic hand. IEEE/ASME Trans Mechatron 25(5):2501–2512
15. Lee HJ, Baik S, Hwang GW, Song JH, Kim DW, Park B, Min H, Kim JK, Koh J, Yang T-H et al (2021) An electronically perceptive bioinspired soft wet-adhesion actuator with carbon nanotube-based strain sensors. ACS Nano 15(9):14137–14148